Ultramicroscopy of Bone at Oral Implant Sites: A Comparison of ED and Control Patients. Part 1—Defining the Protocol

Patcharawan Silthampitag, DDS[a]/Iven Klineberg, MDS, BSc, PhD, FRACDS, FDSRCS[b]/
Allan S. Jones, BAppSc, PhD[c]/Bruce Austin, BDS, MDSc, FRACDS (OMS)[d]/
Kwan Yat Zee, BDS, MDSc, Odont Dr, FCDSHK[e]/Christine Wallace, BDS, MDS, FRACDS[f]/
Stefan Scholz, DDS, PhD Dr Med Dent[g]/Anthony Naim, BDS, MBBS, FRACDS, FRACDS (OMS)[h]/
Khaled Zoud, BDS, BMed, FRACDS (OMS)[h]

Purpose: The aim of this study was to develop a protocol to analyze the microstructure of mandibular and maxillary bone in association with implant placement in ectodermal dysplasia (ED) and anodontia conditions compared to patients not suffering from such conditions. ***Materials and Methods:*** This study was not additionally invasive, since the bone harvesting was completed at the time and site of implant placement. Bone samples were allocated into two groups (ED and control patients) and specified by the site of bone harvesting. Microcomputed tomography (micro-CT) analysis at 5-µm resolution was conducted on each bone sample. Computer analysis applying specialized CT analysis and software allowed evaluation of the three-dimensional microstructure of alveolar and basal bone samples for comparison of structural parameters. ***Results:*** Ten bone samples (five alveolar and five basal) were harvested. Preliminary data confirmed the structural features and significant differences between alveolar and basal bone. Basal bone had greater absolute and percent bone volume, greater bone surface, and a lower trabecular bone pattern factor than alveolar bone. ***Conclusion:*** Preliminary data were derived from bone harvested from both the maxilla and mandible of control patients, while bone samples from ED patients were harvested from only the anterior mandible. Further bone samples will provide more data on whether broader areas of bone harvesting, age, or sex affect the quality and quantity of the bone and influence implant treatment outcomes. *Int J Prosthodont 2011;24:147–154.*

[a]*Graduate Student, Professorial Unit, Faculty of Dentistry, The University of Sydney Westmead Centre for Oral Health, Westmead, Australia.*
[b]*Professor and Chair of Oral Rehabilitation, Professorial Unit, Faculty of Dentistry, The University of Sydney, Sydney, Australia.*
[c]*Associate Professor, Image Analysis. Australian Centre for Microscopy & Microanalysis, The University of Sydney, Sydney, Australia.*
[d]*Part-time Lecturer, Department of Oral and Maxillofacial Surgery, The University of Sydney Westmead Centre for Oral Health, Westmead, Australia.*
[e]*Associate Professor, Department of Periodontology, Faculty of Dentistry, The University of Sydney Westmead Centre for Oral Health, Westmead, Australia.*
[f]*Head, Department of Oral Restorative Sciences, Faculty of Dentistry, The University of Sydney Westmead Centre for Oral Health, Westmead, Australia.*
[g]*Associate Professor of Oral Rehabilitation, Faculty of Dentistry, The University of Sydney Westmead Centre for Oral Health, Westmead, Australia.*
[h]*Specialist Oral and Maxillofacial Surgeon, The University of Sydney Westmead Centre for Oral Health, Westmead, Australia.*

Correspondence to: *Prof Iven Klineberg, Professorial Unit, Westmead Centre for Oral Health, Westmead Hospital, NSW 2145, Australia. Fax: (02) 9633 2893. Email: ivenk@mail.usyd.edu.au*

The use of endosseous implants has become a common treatment for the replacement of missing teeth since Brånemark and colleagues documented the predictability and successful outcomes of such treatment.[1,2] The success has been attributed to osseointegration, which is understood to be the direct structural and functional connection between living bone and the surface of a loaded implant.[3,4] Notwithstanding this success, implant failures continue to be reported. It has been suggested that available bone quantity and quality at an implant site significantly influence osseointegration and implant survival and, therefore, are important considerations in treatment planning.[5]

Attempts have been made to classify bone quality to assist in the selection of appropriate site-specific implants and surgical procedures and to predict outcomes. Lekholm and Zarb[6] developed a working classification of jawbone type to facilitate case planning. They proposed a differentiation of jawbone quantity, shape, and quality, based on quality defined as types 1 to 4 and quantity defined as types A to E.

Bone quality types 1 and 2 are representative of the mandible, while types 3 and 4 are observed primarily in the maxilla.[7] Jaffin and Berman[8] described the total implant failure rate in a 5-year analysis as 3% in bone quality types 1, 2, and 3 and 35% in type 4. Lindh et al[9] and Parfitt et al[10] reported data of particular relevance to this study: Jawbone trabeculae vary in shape, size, and thickness. The mandible is recognized as having thicker cortical and denser trabecular bone compared with the maxilla, and in both the maxilla and mandible, the posterior region trabecular structure is poorer than in the anterior region.[7,9] Esposito et al[11] reported that the cortical bone in both arches becomes thinner and more porous posteriorly. These observations emphasize the importance of bone structure in implant surgery, especially in the maxilla, where primary implant stability may be difficult to achieve.

In ectodermal dysplasia (ED) patients with hypodontia or anodontia, the absence of teeth compromises jawbone growth and may further influence the potential for implant osseointegration. Management of ED patients with implant treatment is advocated universally, and current data is encouraging. Further studies of bone quality and quantity in relation to osseointegration in ED patients may provide data relevant to evaluation of treatment possibilities and outcomes.

Evaluation of bone quality and quantity includes radiographic imaging and surgical assessment at the time of implant placement. More recently, microcomputed tomography (micro-CT) has emerged as a highly accurate and nondestructive method for analysis of the bone microstructure.[12–15] Micro-CT technology has improved spatial resolution and enables accurate geometric determination of the bone microstructure. As a result, it has become more acceptable for acquisition of bone images for treatment planning to specify bone detail for implant placement.[16] With a resolution of less than 10 μm,[17] micro-CT provides three-dimensional (3D) reconstructed images with the possibility of deriving information on detailed morphology and bone density. Micro-CT analysis on bone architecture has been shown to correlate with the mechanical properties of bone.[18–20] A recent study analyzed in vitro data from human cadavers,[21] but to date there is little clinical data. An in vivo study to develop a microtomography technique to determine bone structure surrounding implants prepared bone samples from retrieved microimplants; however, there were limited samples and the accuracy of the technique needs evaluation.[22]

The aim of this study was to analyze the microstructure of mandibular and maxillary bone in association with implant placement. The general hypothesis was that receiving more detailed information on bone structure had the potential to improve the clinical protocol for implant management (diagnosis and treatment planning) and, thus, outcomes of ED and hypodontia conditions. A further hypothesis was that distinct differences in bone volume and bone mineral density in different regions of the jawbone and between patients with and without ED would influence implant treatment outcomes.

Materials and Methods

Participants were recruited from patients receiving implant treatment at the Department of Oral Restorative Sciences, The University of Sydney Westmead Centre for Oral Health, Westmead, Australia. Subjects were allocated into two patient groups (patients with and without [control] ED) and ranged in age from 14 to 70 years. Selection of control and ED patients was made at random from a larger subset. Participants with a medical history including diabetes, osteoporosis, cancer treatment (radiation treatment and chemotherapy), use of corticosteroids, and participants who were current smokers were excluded.

ED patients were diagnosed as either hidrotic or hypohidrotic based on the severity of the condition. Less common forms of ED (eg, X-linked osteopetrosis, lymphedema, anhidrotic ED and immunodeficiency [OLEDAID]) were not found in this study.

Dental assessments were carried out primarily by prosthodontic specialists and prosthodontic postgraduate students to document, among other things, the adequacy of residual bone contour and volume, interocclusal distance, condition of any remaining teeth, periodontal status, and oral hygiene for determining an appropriate management plan, including use of implants. Participants who required bone grafting prior to or associated with implant treatment were excluded from this study.

Patients who satisfied the inclusion criteria were referred for imaging (cone beam volumetric tomography, manipulated with NobelGuide [Nobel Biocare] software, and orthopantomogram) following diagnostic preparation and construction of a radiographic guide. Detailed treatment planning was then completed.

Bone Specimens

This study was approved by the ethics committee of Sydney West Area Health Service Human Research Ethics Committees, Westmead Campus, and The University of Sydney, Australia. Appropriate informed consent, both oral and written, was obtained from participants. One clinician described and answered

questions from each patient about the study. With patients under 18 years of age, informed consent was received from their parents or guardians.

At the time of implant placement, a bone sample 2 to 3 mm in diameter and approximately 5 mm in length was harvested from the implant site of all patients (Fig 1), and implants with a diameter of 3.75 mm or greater were placed following the defined and recognized protocol. A trephine bur with an internal diameter of 2 to 3 mm was used to harvest bone samples without harming the implant site, given the relative sizes of the bone sample and implant. It was believed that with very careful handling of the trephine to minimize any pressure and with slow rotation and sterile saline cooling, the sampling procedure would not influence the quality of the bone harvested. There did not appear to be any rotational drag at the margins of the specimens.

The age range of control patients was 32 to 64 years, and that of ED patients was 14 to 20 years. Dental history data of the control patients did not identify the date of tooth extraction in the area of implant placement, whereas two of five ED patients presented without any teeth, and bone was sampled as described from the implant site. Three ED patients had teeth extracted at the time of implant placement, and in such instances, bone samples were harvested from the area immediately adjacent to the extraction sites.

Participants were treated following an identical protocol as regular implant patients not included in the study. There were no additional risks apart from the low, but accepted, possible risk of implant failure—a feature of all implant treatments.

Harvested bone was derived from bone that would be removed during routine implant placement, and no additional bone was removed. Bone samples were stored in 4% formaldehyde and refrigerated. During transportation, samples were carried in a specimen container surrounded by a cold pack.

Micro-CT Imaging

Each specimen was stabilized with plastic foam within a plastic straw of greater diameter than the bone sample. A wet cotton plug covered with dental wax was placed around the straw to maintain the moisture content of the bone sample during scanning.

Bone samples were scanned with a resolution of 5 µm using a SkyScan 1172 high-resolution desktop x-ray microtomography system (SkyScan) to obtain 3D microstructural information.[23] The scan protocol included rotation through 360 degrees with x-ray settings standardized to 60 kV and 160 µA. The beam was projected onto a phosphorus screen, which converted the x-rays into visible light and was detected by a charge-coupled device. Data were digitized and transmitted to a computer with tomographic reconstruction software. A rotation of 0.2 degrees and an exposure time of 1.18 seconds were used between image acquisitions, providing a series of approximately 1,800 images.[24–26]

Fig 1 Bone sample 2 to 3 mm in diameter and approximately 5 mm in length.

Computer software (ConeRec version 2.13, SkyScan) was used to create the 3D model and analyze the reconstruction of bone samples. The 16-bit TIFF image generated raw reconstructed axial slices by applying a reconstruction algorithm. Individual axial slices were generated as bitmap images with an 8-bit grayscale dynamic range. The gray values in each data set were calibrated so that the 8-bit range mapped the variation between the pixels with maximum x-ray attenuation (the most opaque: 255) and those with minimum x-ray attenuation (transparent: 0) completely.[26]

VGStudiomax 1.1 software (Volume Graphics) was used for the 3D reconstruction of each bone sample and allowed all aspects of the scanned specimen to be visualized.

After reconstructing the image, the volume of interest (VOI) in each bone sample was measured from the middle of the specimen to 1 mm on both sides to generate representative and meaningful data (Fig 2a). To obtain a cross-sectional image set, a 2-mm-diameter circular region of interest (ROI) was drawn on all slices (Fig 2b). Specialized CT analysis software was applied to analyze the 3D microstructure of the bone samples and compared 10 structural parameters for the different groups: bone volume (BV), percent bone volume (BV/TV), bone surface (BS), bone specific surface

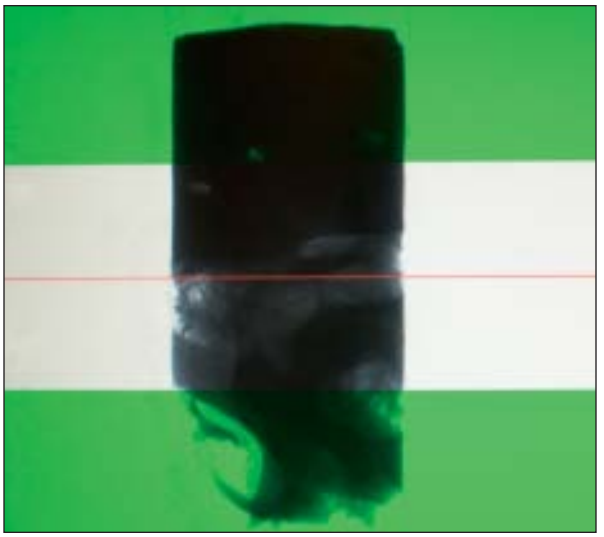

Fig 2a VOI measured from the middle of the specimen to 1 mm on both sides of the midline.

Fig 2b Circular ROI of the bone specimen with a 2-mm diameter.

(BS/BV), bone surface density (BS/TV), trabecular thickness (TbTh), trabecular separation (TbSp), trabecular number (TbN), trabecular bone pattern factor (TbPf), and Structure Model Index (SMI).

Bone Volume (BV). BV, regarded as the total volume of binarized objects within the VOI,[19] and the Marching Cubes volume model for binarized objects were used to measure the 3D volume within the VOI.

Percent Bone Volume (BV/TV). This 3D parameter relates bone volume to total tissue volume (BV/TV). The value was obtained by adding together the volume of voxels within the triangles into which the 3D surface was divided. The number of voxels within the bone then was divided by the total number of voxels. When this measurement is taken from a 2D image, the bone area can be obtained. This value was below 100% in trabecular bone and close to 100% for cortical bone.[27,28]

Bone Surface (BS). The BS area of the entire solid subject within the VOI was measured in three dimensions.

Bone Specific Surface (BS/BV). This 3D parameter relates the BS to total bone volume and was obtained by triangulation of the trabecular surface. It increases inversely with the number of trabeculae.[27,28]

Bone Surface Density (BS/TV). BS/TV is the ratio of surface area to total volume, measured in three dimensions, within the VOI.

Trabecular Thickness (TbTh), Trabecular Separation (TbSp), and Trabecular Number (TbN). These 2D parameters can be calculated by using the mean intercept length method developed by Whitehouse.[29] A grid of parallel lines was superimposed on the image, and a ratio was obtained between the intersection points of the lines and the bone marrow interface of the trabeculae, in relation to the total gridlines. This method can be used to determine TbSp and TbTh, but it is not valid for 3D assessment. The three variables are obtained directly from a 3D image by computer measurement in each voxel by the localization of spheres within and among trabeculae.[30]

Trabecular Bone Pattern Factor (TbPf). This index was developed by Hahn et al[31] and describes the connectedness of individual trabeculae in each 2D section. The basic idea is that the connectedness of the structure may be described by the relation of convex to concave surfaces. A high number of convex surfaces represents a poorly connected structure, while a high number of concave surfaces represents a well-connected structure. TbPf leads to low values where there is well-connected trabecular bone, whereas a preponderance of isolated trabeculae results in high values of the TbPf.

Structural Model Index (SMI). This variable indicates the prevalence of rodlike or platelike components of the trabeculae and may be obtained by differential analyses of the triangulated surface of a 3D structure using a mathematic model. It is quantified from level 0 (platelike) to 3 (rodlike), as described by Hildebrand and Rüegsegger[32] and Cano et al.[33]

Statistical Analysis

The mean value and standard deviation of each parameter were calculated for the alveolar and basal bone groups. The Student *t* test was used to compare the parameters between the two groups, with significance accepted at $P < .05$.

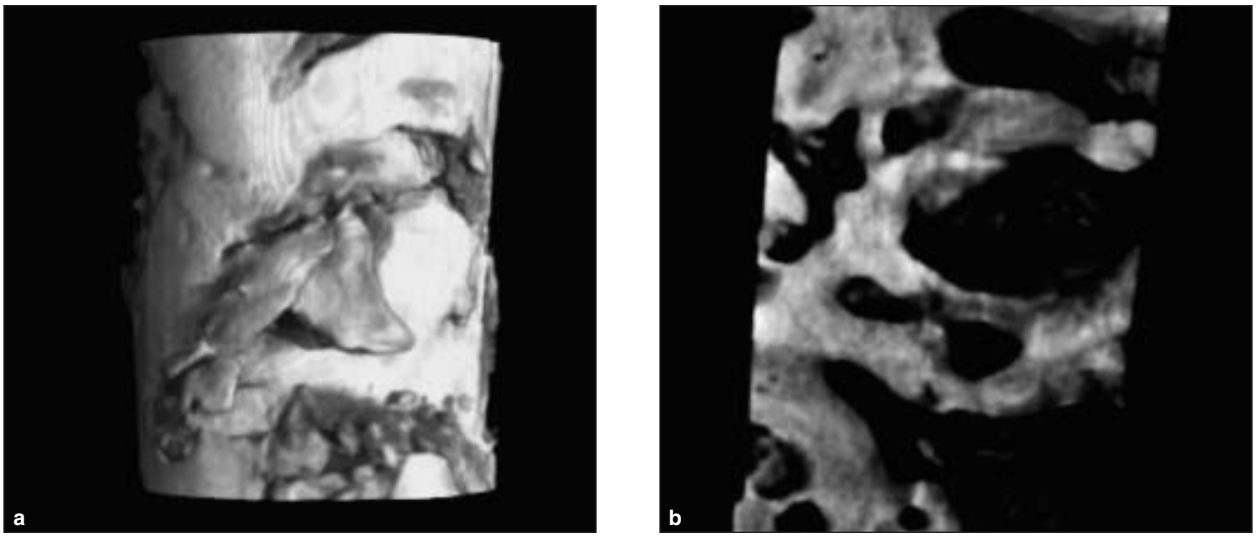

Figs 3a and 3b VOI of bone harvested from an ED patient (2-mm diameter, 2-mm length).

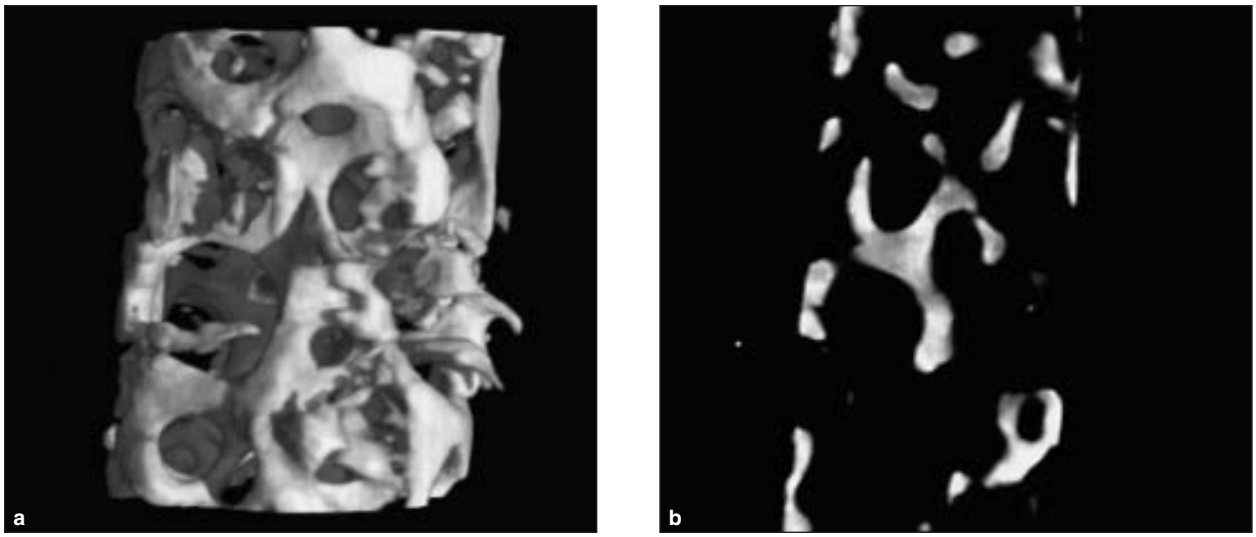

Figs 4a and 4b VOI of bone harvested from a control patient (2-mm diameter, 2-mm length).

Results

Ten bone samples were harvested from implant patients: five from ED patients (three females, two males) from the anterior mandible and five from control patients (three females, two males) from the posterior areas of the maxilla and mandible. A visual examination of the specimen from 3D reconstruction showed the distinct variation of bone samples harvested from the two groups. In both specimen types, the combination of platelike and rodlike trabeculae was observed. However, bone specimens from the ED group had a denser, more compact, and well-connected structure than specimens from the control group. The latter had a smaller bone volume and fewer and thinner trabeculae with wider spaces between (Figs 3 and 4).

Table 1 details the values of each parameter measured from the two groups. The mean values from each parameter indicated that bone from the ED group had a greater BV, BV/BV, BS, BS/TV, TbTh, TbSp, and TbN. Control specimens had greater BS/TV, TbPf, and SMI than ED specimens (Table 2).

BV, BV/TV, and BS/BV had widely ranging values with significant differences between the two groups. Bone harvested from the ED group had a more compact structure, which may show greater resistance to external force transfer through mastication compared to the control group.

Table 1 Details of Parameter Analyses of Bone Samples Obtained from ED and Control Patients

Region of harvested bone	BV (mm^3)	BV/TV (%)	BS (mm^2)	BS/BV (mm^{-1})	BS/TV (mm^{-1})	TbTh (mm)	TbSp (mm)	TbN (mm^{-1})	TbPf (mm^{-1})	SMI
ED (n = 5)										
Mandible										
Anterior	3.71	59.20	94.49	25.50	15.09	0.16	0.25	3.79	–96.63	–11.14
Anterior	3.91	49.94	42.25	10.81	5.40	0.35	0.28	1.43	–19.27	–3.22
Anterior	4.39	69.69	41.94	9.55	6.66	0.43	0.26	1.60	–9.23	1.79
Anterior	3.40	53.96	43.62	12.82	6.92	0.17	0.47	3.10	–54.01	–22.40
Anterior	3.48	54.88	36.02	10.33	5.67	0.33	0.51	1.66	–3.42	0.48
Control (n = 5)										
Mandible										
Posterior	2.91	46.51	43.08	14.98	6.87	0.24	0.27	1.90	1.78	2.34
Posterior	2.20	34.93	62.34	28.30	9.88	0.20	0.27	1.72	–23.94	0.22
Posterior	1.99	31.54	58.22	29.17	9.29	0.20	0.31	1.56	–4.96	2.72
Maxilla										
Posterior	2.87	45.83	54.01	28.08	8.54	0.16	0.28	1.86	6.22	1.93
Posterior	0.76	12.98	25.37	33.24	4.31	0.14	0.45	1.94	20.73	4.03

BV = bone volume; BV/TV = percent bone volume; BS = bone surface; BS/BV = bone specific surface; BS/TV = bone surface density; TbTh = trabecular thickness; TbSp = trabecular separation; TbN = trabecular number; TbPf = trabecular bone pattern factor; SMI = Structure Model Index.

Table 2 Parametric Values of Bone Specimens Harvested from Control and ED Patients

Bone structural parameters	Mean		SD		Minimum		Maximum		
	Control	ED	Control	ED	Control	ED	Control	ED	*t*
BV (mm^3)	2.15	3.78	0.87	0.40	0.76	3.40	2.91	4.39	0.01
BV/TV (%)	34.36	57.53	13.64	7.55	12.98	49.94	43.51	69.69	0.02
BS (mm^2)	48.60	51.66	14.84	24.12	25.37	36.02	62.34	94.49	0.82
BS/TV (mm^{-1})	26.75	13.80	6.90	6.65	14.98	9.55	33.24	25.50	0.02
BS/BV (mm^{-1})	7.78	7.95	2.24	4.04	4.31	5.40	9.88	15.09	0.94
TbTh (mm)	0.19	0.29	0.04	0.12	0.14	0.16	0.24	0.43	0.13
TbSp (mm)	0.32	0.35	0.08	0.13	0.27	0.25	0.45	0.51	0.58
TbN (mm^{-1})	1.80	2.32	0.16	1.06	1.56	1.43	1.94	3.79	0.34
TbPf (mm^{-1})	–0.03	–36.51	16.35	38.91	–23.94	–96.63	20.73	–3.42	0.11
SMI	2.25	-6.90	1.38	10.02	0.22	–22.40	4.03	1.79	0.11

SD = standard deviation; see Table 1 for parameter acronyms.

There were wide-ranging differences in TbPf and SMI, which quantitatively describes the ratio of inter-trabecular connectivity. Low values of these parameters were found in the ED group, which reflected that bone samples from ED patients presented higher trabecular connectedness than samples from control patients.

Instrument and specimen variance were found in this pilot study. To overcome instrument variance, the optimal gray value in each specimen was calibrated by determining a range of values, which were selected by one researcher based on their experience with the analyses. On average, five measurements were made at the specific sites selected and analyzed to eliminate specimen variance. Six bone samples were selected randomly and rescanned to verify reproducibility (three control, three ED). Each specimen was analyzed five times by moving the VOI up 5 sections from the middle of the specimen and 5 and 10 sections on either side of the midline. Table 3 reports the results with the average values of each bone sample from the first and second scanning.

Discussion

Generally, it has been suggested that bone quality is the major determinant for implant success.[8] Higher bone quality would therefore ensure better implant stability and, consequently, better conditions for successful long-term implant outcomes. As a result, several 2D and 3D measuring techniques have been developed to evaluate bone quality, especially of the trabecular bone structure, which defines the biomechanical property of bone.

A medical CT scanner with a maximum resolution of 250 μm would be unsuitable for imaging individual trabeculae, which can be less than 100 μm in diameter.[34,35] However, micro-CT provides high-resolution images of less than 10 μm. In this study, bone specimens were scanned at a resolution of 5 μm, which is of value for determining the structural and biomechanical features of individual trabeculae. Data from in vitro CT assessments of trabecular bone would assist in the assessment of the structural bone properties. The 3D parameters of trabeculae, including the connectivity and shape, are particularly helpful in analyzing bone quality and, possibly, implant outcomes. Micro-CT operates similarly to clinical CT, but rather than rotating the x-ray source and detectors as in clinical CT, the specimen itself is rotated.

However, micro-CT has some limitations: the equipment is very expensive, access is limited, and specialization is needed to operate the system. In addition, the scanning and reconstruction of specimens consume computer time. However, the technique has been applied to various aspects of dental research and may be productively applied to determine the biomechanical features of bone in relation to implant outcomes.

This preliminary data was derived from bone from control patients harvested variably from both the maxilla (n = 2) and mandible (n = 3), whereas bone samples from ED patients were harvested only from the anterior mandible (n = 5). Visual examination of the structure indicated that bone harvested from ED patients showed thick, well-connected trabeculae and more compact structures than bone from control patients. Structural parameters from ED patients consisted mainly of plate-like structures, which defined well-connected trabeculae, whereas isolated or rodlike trabeculae were found in bone from the control group.

This pilot study suggests that bone from ED patients has an optimal structure to resist occlusal loads. However, only 10 samples were investigated. The various areas of bone harvested, as well as the sex, age, and dental status of patients, may affect the quality of bone. Further analyses with a larger sample size may indicate whether other factors affect bone quality and quantity, as well as implant outcome.

Table 3 Comparison of First and Second Scanning for Average Parameters from Bone Analyses

Bone sample	BV (mm^3)		BV/TV (%)		BS (mm^2)		BS/BV (mm^{-1})		BS/TV (mm^{-1})		TbTh (mm)		TbSp (mm)		TbN (mm^{-1})		TbPf (mm^{-1})		SMI	
	1st	2nd	1st	2nd	1st	2nd	1st	2nd	1st	2nd	1st	2nd	1st	2nd	1st	2nd	1st	2nd	1st	2nd
1 (ED)	3.48	2.64	54.87	41.59	35.99	89.55	10.33	33.84	5.56	14.07	0.33	0.20	0.51	0.44	1.66	2.10	–3.46	–47.78	0.46	–0.89
2 (ED)	4.39	4.29	69.69	68.18	41.93	63.73	9.49	14.86	6.66	10.28	0.43	0.15	0.26	0.23	1.60	4.54	–8.22	–55.40	1.80	–16.54
3 (ED)	3.40	3.22	53.98	51.40	43.51	57.30	12.82	17.80	6.92	9.15	0.37	0.16	0.47	0.47	3.14	3.23	–53.99	–81.15	–22.42	–17.89
4 (control)	2.88	3.06	45.79	48.43	43.18	47.90	15.00	14.74	6.87	7.62	0.24	0.27	0.27	0.54	1.90	1.50	1.84	0.20	2.37	2.97
5 (control)	2.92	3.05	45.89	48.04	45.66	61.73	15.69	20.25	7.30	9.73	0.29	0.25	0.27	0.26	1.57	1.89	–0.36	–9.27	2.09	0.89
6 (control)	2.20	2.64	34.91	42.26	61.32	50.57	28.30	19.13	9.88	8.09	0.20	0.30	0.27	0.40	1.72	–1.42	–23.93	–9.63	0.23	1.93

See Table 1 for parameter acronyms.

Conclusion

The preliminary data identified differences in bone microstructure between ED and control patients. Bone samples from ED patients had significantly higher BV, BV/TV, and BS and lower SMI than bone samples from control patients. These data indicate that bone from ED patients has a more detailed bone structure than bone from control patients. The influence on implant treatment outcomes will be determined as part of a long-term monitoring of these patients.

References

1. Adell R, Lekholm U, Rockler B, Brånemark PI. A 15-year study of osseointegrated implants in the treatment of the edentulous jaw. Int J Oral Surg 1981;10:387–416.
2. Brånemark PI, Adell R, Albrektsson T, Lekholm U, Lundkvist S, Rockler B. Osseointegrated titanium fixtures in the treatment of edentulousness. Biomaterials 1983;4:25–28.
3. Davies JE. Mechanisms of endosseous integration. Int J Prosthodont 1998;11:391–401.
4. Davies JE. Understanding peri-implant endosseous healing. J Dent Educ 2003;67:932–949.
5. Duyck J, Naert I. Failure of oral implants: Aetiology, symptoms and influencing factors. Clin Oral Investig 1998;2:102–114.
6. Lekholm U, Zarb GA. Patient selection and preparation. In: Brånemark P-I, Zarb GA, Albrektsson T (eds). Integrated Prostheses: Osseointegration in Clinical Dentistry. Chicago: Quintessence, 1985:109–209.
7. Ulm C, Kneissel M, Schedle A, et al. Characteristic features of trabecular bone in edentulous maxillae. Clin Oral Implants Res 1999;10:459–467.
8. Jaffin RA, Berman CL. The excessive loss of Brånemark fixtures in type IV bone: A 5-year analysis. J Periodontol 1991;62:2–4.
9. Lindh T, Gunne J, Tillberg A, Molin M. A meta-analysis of implants in partial edentulism. Clin Oral Implants Res 1998; 9:80–90.
10. Parfitt AM, Drezner MK, Glorieux FH, et al. Bone histomorphometry: Standardization of nomenclature, symbols, and units. Report of the ASBMR Histomorphometry Nomenclature Committee. J Bone Miner Res 1987;2:595–610.
11. Esposito M, Hirsch JM, Lekholm U, Thomsen P. Biological factors contributing to failures of osseointegrated oral implants. (II). Etiopathogenesis. Eur J Oral Sci 1998;106:721–764.
12. Nazarian A, Snyder BD, Zurakowski D, Müller R. Quantitative micro-computed tomography: A non-invasive method to assess equivalent bone mineral density. Bone 2008;43:302–311.
13. Efeoglu C, Fisher SE, Ertürk S, Oztop F, Günbay S, Sipahi A. Quantitative morphometric evaluation of critical size experimental bone defects by microcomputed tomography. Br J Oral Maxillofac Surg 2007;45:203–207.
14. Stauber M, Müller R. Micro-computed tomography: A method for the non-destructive evaluation of the three-dimensional structure of biological specimens. Methods Mol Biol 2008;455:273–292.
15. Barou O, Valentin D, Vico L, et al. High-resolution three-dimensional micro-computed tomography detects bone loss and changes in trabecular architecture early: Comparison with DEXA and bone histomorphometry in a rat model of disuse osteoporosis. Invest Radiol 2002;37:40–46.
16. Hanson NA, Bagi CM. Alternative approach to assessment of bone quality using micro-computed tomography. Bone 2004; 35:326–333.
17. Ito M. Assessment of bone quality using micro-computed tomography (micro-CT) and synchrotron micro-CT. J Bone Miner Metab 2005;23(suppl):115–121.
18. Dempster DW. Bone microarchitecture and strength. Osteoporos Int 2003;14(suppl 5):S54–56.
19. Moon HS, Won YY, Kim KD, et al. The three-dimensional microstructure of the trabecular bone in the mandible. Surg Radiol Anat 2004;26:466–473.
20. van der Linden JC, Weinans H. Effects of microarchitecture on bone strength. Curr Osteoporos Rep 2007;5:56–61.
21. Aranyarachkul P, Caruso J, Gantes B, et al. Bone density assessments of dental implant sites: 2. Quantitative cone-beam computerized tomography. Int J Oral Maxillofac Implants 2005; 20:416–424.
22. Sennerby L, Wennerberg A, Pasop F. A new microtomographic technique for non-invasive evaluation of the bone structure around implants. Clin Oral Implants Res 2001;12:91–94.
23. Jones AS, Reztsov A, Loo CE. Application of invariant grey scale features for analysis of porous minerals. Micron 2007; 38:40–48.
24. Fanuscu MI, Chang TL. Three-dimensional morphometric analysis of human cadaver bone: Microstructural data from maxilla and mandible. Clin Oral Implants Res 2004;15:213–218.
25. Guggenbuhl P, Bodic F, Hamel L, Baslé MF, Chappard D. Texture analysis of X-ray radiographs of iliac bone is correlated with bone micro-CT. Osteoporos Int 2006;17:447–454.
26. Harris DA, Jones AS, Darendeliler MA. Physical properties of root cementum: Part 8. Volumetric analysis of root resorption craters after application of controlled intrusive light and heavy orthodontic forces: A microcomputed tomography scan study. Am J Orthod Dentofacial Orthop 2006;130:639–647 [erratum 2007;132:277].
27. Müller R. Long-term prediction of three-dimensional bone architecture in simulations of pre-, peri- and post-menopausal microstructural bone remodeling. Osteoporos Int 2005;16 (suppl 2):S25–35.
28. Borah B, Dufresne TE, Ritman EL, et al. Long-term risedronate treatment normalizes mineralization and continues to preserve trabecular architecture: Sequential triple biopsy studies with micro-computed tomography. Bone 2006;39:345–352.
29. Whitehouse WJ. The quantitative morphology of anisotropic trabecular bone. J Microsc 1974;101:153–168.
30. Fajardo RJ, Müller R. Three-dimensional analysis of nonhuman primate trabecular architecture using micro-computed tomography. Am J Phys Anthropol 2001;115:327–336.
31. Hahn M, Vogel M, Pompesius-Kempa M, Delling G. Trabecular bone pattern factor—A new parameter for simple quantification of bone microarchitecture. Bone 1992;13:327–330.
32. Hildebrand T, Rüegsegger P. Quantification of bone microarchitecture with the Structure Model Index. Comput Methods Biomech Biomed Engin 1997;1:15–23.
33. Cano J, Campo J, Vaquero JJ, Martinez JM, Bascones A. High resolution image in bone biology I. Review of the literature. Med Oral Patol Oral Cir Bucal 2007;12:e454–458.
34. Müller R, Hahn M, Vogel M, Delling G, Rüegsegger P. Morphometric analysis of noninvasively assessed bone biopsies: Comparison of high-resolution computed tomography and histologic sections. Bone 1996;18:215–220 [erratum 1996; 19:299].
35. Engelke K, Song S, Glüer C, Genant H. A digital model of trabecular bone. J Bone Miner Res 1996;11:480–489.